# Communication

## On the Stability of the RK-FDTD Method for Graphene Modeling

José A. Pereda and Ana Grande

***Abstract*—The Runge–Kutta finite-difference time-domain (RK-FDTD) method is an extension of the conventional finite-difference time-domain (FDTD) technique to include graphene sheets. According to this method, the relationship between the current density and the electric field for graphene is discretized by applying an explicit second-order Runge–Kutta (RK) scheme. It has recently been concluded that the RK-FDTD method is subject to the same Courant–Friedrichs–Lewy (CFL) stability limit as the conventional FDTD method. This communication revisits the stability analysis of the RK-FDTD method. To this end, the von Neumann method is combined with the Routh–Hurwitz (RH) criterion. As a result, closed-form stability conditions are obtained. It is shown that in addition to the CFL stability limit, the RK-FDTD method must also satisfy new conditions involving graphene parameters. Unfortunately, the RK-FDTD method becomes unstable for commonly used values of these parameters. The theoretical results are confirmed with numerical examples.**

***Index Terms*—Finite-difference time-domain (FD-TD) method, graphene, second-order Runge–Kutta (RK) scheme, stability.**

### I. Introduction

Since graphene was first isolated in 2004, this 2-D material has attracted a great deal of interest in a wide range of fields due to its outstanding properties [1], [2]. From an electromagnetic viewpoint, graphene is characterized by a dispersive surface conductivity [3]. Thus, the study of graphene devices requires the extension of previously available computational electromagnetic tools [4].

The finite-difference time-domain (FDTD) method is one of the most popular numerical techniques for solving Maxwell's equations in the time domain [5]. There are currently two main approaches to include graphene sheets within FDTD simulations. The first one relies on the surface boundary condition (SBC) concept [6]. In the second one, the current density is related to the electric field through an equivalent volumetric conductivity [7], [8], [9], [10].

A finite-difference scheme is stable when numerical rounding errors do not grow unboundedly as the simulation goes on. For the FDTD method to remain stable, the maximum time step size must be limited by the Courant–Friedrichs–Lewy (CFL) condition [5]. Thus, it is crucial to study to what extent the stability of the FDTD method is affected when graphene is included. Recently, stability analyses have been performed for the SBC-FDTD technique [11] and for schemes based on the volumetric conductivity approach [12], [13], [14].

An FDTD scheme for gyrotropic graphene was introduced in [10] and then adapted for isotropic graphene in [14]. This method assumes a Drude-like conductivity for graphene. The resulting relationship between the electric field and the current density is discretized in the time domain by applying an explicit second-order Runge–Kutta (RK) scheme. Thus, we will refer to this technique as the RK-FDTD method. A stability analysis of the RK-FDTD method was carried out in [14] concluding that this technique retains the CFL time-step limit.

Received 25 June 2024; revised 29 April 2025; accepted 8 June 2025. Date of publication 26 June 2025; date of current version 14 October 2025. This work was supported by the Spanish Ministerio de Ciencia e Innovación under Grant PID2022-137619NB-I00. *(Corresponding author: José A. Pereda.)*

José A. Pereda is with the Departamento de Ingeniería de Comunicaciones (DICOM), Universidad de Cantabria, 39005 Santander, Spain (e-mail: peredaj@unican.es).

Ana Grande is with the Departamento de Electricidad y Electrónica, Universidad de Valladolid, 47011 Valladolid, Spain (e-mail: anamaria.grande@uva.es).

Digital Object Identifier 10.1109/TAP.2025.3581386

This communication revisits the stability analysis of the RK-FDTD method. To achieve this goal, the von Neumann method is used in conjunction with the Routh–Hurwitz (RH) criterion [15]. As a result, stability conditions are obtained in closed-form for the RK-FDTD method. Specifically, we find that jointly to the CFL stability limit, the RK-FDTD method must also satisfy new conditions involving graphene parameters. Unfortunately, the RK-FDTD method becomes unstable for commonly used values of these parameters. Based on our experience, the instability is present throughout the entire simulation, but it typically manifests after the initial transient response has settled. It often becomes more apparent when the simulation is well into the late-time region of the time evolution. This behavior is usually referred to as a late-time instability.

### II. Governing Equations

The time-dependent Maxwell curl equations in an isotropic graphene sheet can be expressed as

$$\mu_0 \frac{\partial \vec{H}}{\partial t} = -\nabla \times \vec{E} \tag{1a}$$

$$\varepsilon_0 \frac{\partial \vec{E}}{\partial t} = \nabla \times \vec{H} - \vec{J} \tag{1b}$$

where $\varepsilon_0$ and $\mu_0$ are the free-space permittivity and permeability, respectively.

For frequencies up to 10 THz and considering the graphene sheet as a volumetric material, the current density is related to the electric field, in the frequency domain, by the following Drude-like constitutive relation:

$$\vec{J}(\omega) = \frac{1}{d} \frac{\sigma_0}{1 + j\omega\tau} \vec{E}(\omega) \tag{2}$$

where $d$ is the thickness of the graphene sheet and $\sigma_0$ is given by

$$\sigma_0 = \frac{e^2 \tau k_B T}{\pi \hbar^2} \left\{ \frac{\mu_c}{k_B T} + 2 \ln \left[ \exp\left( \frac{-\mu_c}{k_B T} \right) + 1 \right] \right\}$$

with $\tau$ being the electron relaxation time, $\mu_c$ the chemical potential, $T$ the temperature, $-e$ the electron charge, $k_B$ the Boltzmann's constant, and $\hbar$ the reduced Planck's constant.

Considering the transformation $j\omega \leftrightarrow d/dt$, (2) can be expressed in the time domain as the following first-order ordinary differential equation:

$$\tau \frac{d\vec{J}}{dt} + \vec{J} = \sigma_d \vec{E} \tag{3}$$

where $\sigma_d = \sigma_0/d$. In Section III, we discuss the discretization of (1) and (3) using the RK-FDTD method.

### III. RK-FDTD Method

According to the conventional FDTD method [5], Faraday's equation in (1a) is approximated at $t = n\Delta_t$ as

$$\vec{H}^{n+\frac{1}{2}} = \vec{H}^{n-\frac{1}{2}} - \frac{\Delta_t}{\mu_0} \nabla \times \vec{E}^n \tag{4}$$

where $\Delta_t$ is the time step. Analogously, Ampère's law in (1b) is discretized at $t = (n + (1/2))\Delta_t$ as

$$\vec{E}^{n+1} = \vec{E}^n + \frac{\Delta_t}{\varepsilon_0} \nabla \times \vec{H}^{n+\frac{1}{2}} - \frac{\Delta_t}{2\varepsilon_0} \left( \vec{J}^{n+1} + \vec{J}^n \right) \tag{5}$$

where the current density term has been approximated using time averaging. The same spatial discretization as in the conventional FDTD method is assumed in (4) and (5), [5].

Based on the RK-FDTD method [14], (3) is approximated by applying an explicit second-order RK scheme, leading to

$$\vec{J}^{n+1} = a_1 \vec{J}^{n} + a_2 \vec{E}^{n} \tag{6}$$

where

$$a_1 = 1 - \frac{1}{\bar{\tau}}\left(1 - \frac{1}{2\bar{\tau}}\right) \tag{7a}$$

$$a_2 = \frac{\sigma_d}{\bar{\tau}}\left(1 - \frac{1}{2\bar{\tau}}\right) \tag{7b}$$

with $\bar{\tau} = \tau/\Delta_t$. In (5) and (6), $\vec{J}$ and $\vec{E}$ are collocated in space and time.

Note that (6) is a fully explicit expression for updating $\vec{J}$ at each time step. This feature makes the application of the RK-FDTD method to gyrotropic graphene simpler than using other non fully explicit schemes [10].

## IV. Stability Analysis

In this section, the stability of the RK-FDTD method is studied by combining the von Neumann technique with the RH criterion [15]. Starting from the governing difference equations (4)–(6), and following the procedure described in [15], we arrive at the stability polynomial $S(Z)$ given by

$$S(Z) = \left[(Z-1)^2 + 4\nu^2 Z\right](Z - a_1) + \frac{a_2\Delta_t}{2\varepsilon_0}\left(Z^2 - 1\right) \tag{8}$$

where the coefficients $a_{1,2}$ have been given in (7) and $\nu = \Delta_t/\Delta_{t,\max}^{\mathrm{CFL}}$ is the CFL number, with $\Delta_{t,\max}^{\mathrm{CFL}}$ being the largest stable time step permitted by the CFL stability limit, given by [5]

$$\Delta_{t,\max}^{\mathrm{CFL}} = \frac{1}{c}\left(\frac{1}{\Delta_x^2} + \frac{1}{\Delta_y^2} + \frac{1}{\Delta_z^2}\right)^{-\frac{1}{2}} \tag{9}$$

where $\Delta_\alpha$ is the size of the spatial cell in the $\alpha$-direction, and $c$ is the speed of light in free space.

According to the von Neumann method, to ensure stability all the roots $Z_i$ of the polynomial $S(Z)$ must lie inside or on the unit circle in the complex $Z$ plane, i.e., $|Z_i| \le 1\ \forall i$. The root-locus method was used in [14] to investigate the location of the roots of the stability polynomial S(Z). Alternatively, the RH criterion is used here. To this end, the bilinear transformation

$$Z = \frac{r+1}{r-1}$$

is first applied to the polynomial $S(Z)$ in (8), resulting in a new polynomial $S(r)$ in the $r$ plane given by

$$S(r) = b_0 r^3 + b_1 r^2 + b_2 r + b_3 \tag{10}$$

where

$$b_0 = \frac{\nu^2}{2\bar{\tau}}\left(1 - \frac{1}{2\bar{\tau}}\right) \tag{11a}$$

$$b_1 = \nu^2\left[\left(1 - \frac{1}{2\bar{\tau}}\right)^2 + \frac{1}{2\bar{\tau}}\right] + \frac{\sigma_d\Delta_t}{4\varepsilon_0\bar{\tau}}\left(1 - \frac{1}{2\bar{\tau}}\right) \tag{11b}$$

$$b_2 = \frac{1}{2\bar{\tau}}\left(1 - \frac{1}{2\bar{\tau}}\right)\left[\left(1 - \nu^2\right) - \frac{\sigma_d\Delta_t}{2\varepsilon_0}\right] \tag{11c}$$

$$b_3 = \left(1 - \nu^2\right)\left[\left(1 - \frac{1}{2\bar{\tau}}\right)^2 + \frac{1}{2\bar{\tau}}\right]. \tag{11d}$$

This transformation maps the exterior of the unit circle in the $Z$ plane onto the right-half side of the $r$ plane. Thus, the stability condition is now that $S(r)$ must have no roots in the right-half side of the $r$ plane. Routh's table is then built up for $S(r)$, and the stability conditions are found by enforcing the entries of the first column of this table to be nonnegative quantities.

Routh's table for the polynomial $S(r)$ in (10) is

| | |
|---|---|
| $c_{1,0} = b_0$ | $b_2$ |
| $c_{2,0} = b_1$ | $b_3$ |
| $c_{3,0} = \frac{b_1 b_2 - b_0 b_3}{b_1}$ | 0 |
| $c_{4,0} = b_3$ | 0 |

Enforcing $c_{1,0} \ge 0$ leads to the condition $1 - 1/(2\bar{\tau}) \ge 0$. In addition, it is easy to see that $c_{2,0} \ge 0$ is met provided that $c_{1,0} \ge 0$ is fulfilled.

For $c_{3,0}$ to be nonnegative, we enforce $b_1 b_2 - b_0 b_3 \ge 0$, which results in the following additional condition:

$$\frac{1}{2\bar{\tau}}\left(1 - \frac{1}{2\bar{\tau}}\right)\left(1 - \frac{\sigma_d\Delta_t}{2\varepsilon_0}\right) - \nu^2 \ge 0.$$

Finally, $c_{4,0} \ge 0$ leads to $\nu^2 \le 1$. For this condition, the case $\nu^2 = 1$ deserves particular attention.

For $\nu^2 = 1$, the polynomial $S(r)$ in (10) reduces to

$$S(r)|_{\nu^2=1} = r\left(r^2 b_0 + r b_1 + b_2\right)\big|_{\nu^2=1}$$

where the coefficients $b_{0,1,2}$ have been given in (11). Routh's table for the polynomial inside parentheses is

| | |
|---|---|
| $\frac{1}{2\bar{\tau}}\left(1 - \frac{1}{2\bar{\tau}}\right)$ | $-\left(1 - \frac{1}{2\bar{\tau}}\right)\frac{\sigma_d\Delta_t}{4\bar{\tau}\varepsilon_0}$ |
| $\frac{1}{2\bar{\tau}} + \left(1 - \frac{1}{2\bar{\tau}}\right)^2 + \frac{\sigma_d\Delta_t}{4\bar{\tau}\varepsilon_0}\left(1 - \frac{1}{2\bar{\tau}}\right)$ | 0 |
| $-\left(1 - \frac{1}{2\bar{\tau}}\right)\frac{\sigma_d\Delta_t}{4\bar{\tau}\varepsilon_0}$ | 0 |

Clearly, there is always a sign change in the first column of the above table, and therefore, the case $\nu^2 = 1$ is unstable.

Summarizing, the stability conditions for the RK-FDTD method are

$$1 - \frac{1}{2\bar{\tau}} \ge 0 \tag{12a}$$

$$F(\nu) = \frac{1}{2\bar{\tau}}\left(1 - \frac{1}{2\bar{\tau}}\right)\left(1 - \frac{\sigma_d\Delta_t}{2\varepsilon_0}\right) - \nu^2 \ge 0 \tag{12b}$$

$$\nu^2 < 1. \tag{12c}$$

According to (12c), the RK-FDTD method must satisfy the CFL condition in a strict sense, i.e., the case $\nu^2 = 1$ is unstable. Moreover, the choice of a stable time step depends on graphene parameters, as shown in (12a) and (12b). In particular, the condition (12b) is very restrictive, making the RK-FDTD method unstable in practice. This idea is illustrated with the following example.

We consider a working frequency $f = 10$ THz. The FDTD cell size is $\Delta_x = \Delta_y = \Delta_z = \Delta = \lambda/N_\lambda$, where $\lambda$ is the wavelength in free space and $N_\lambda$ is the number of cells per wavelength. The graphene parameters are $\tau = 0.5$ ps, $\mu_c = 0.5$ eV, $T = 300$ K, and $d = \Delta$. Fig. 1 shows plots of the left-hand side (LHS) of inequality (12b) as a function of the CFL number $\nu$ for several values of $N_\lambda$. It can be seen that the LHS of (12b) is negative across the entire range of $\nu$ for all the considered spatial resolutions. Therefore, for this example, the RK-FDTD method is unstable.

## V. Simulation Examples

As an application example, we consider the 1-D RK-FDTD simulation of a Gaussian plane wave propagating in free space along the z-direction and impinging normally on an infinite graphene sheet. The simulation domain has 1000 spatial cells and is terminated with absorbing boundary conditions. The graphene sheet is located in the middle of the simulation domain. The maximum effective frequency of the Gaussian pulse is $f_{\max} = 1$ THz. The spatial step is $\Delta_z = \lambda_{\min}/100 \simeq 3\ \mu$m, where $\lambda_{\min}$ is the minimum wavelength in free space, i.e., $\lambda_{\min} = c/f_{\max}$. The graphene parameters are $\tau = 0.5$ ps, $\mu_c = 0.5$ eV, $T = 300$ K, and $d = \Delta_z$. For this

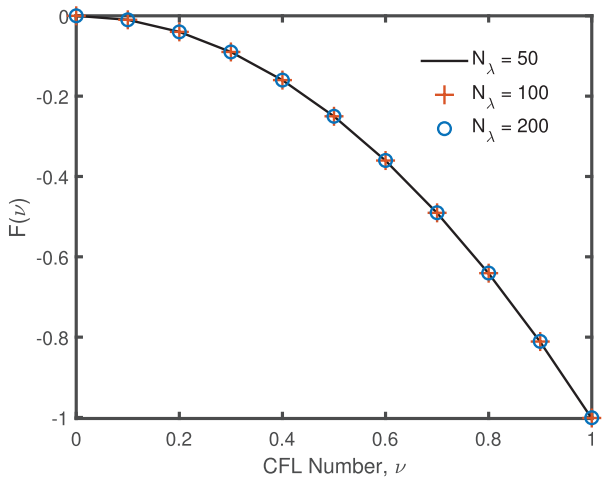


Fig. 1. LHS of the stability condition (12b) versus the CFL number for several spatial resolutions. Stability requires $F(\nu) \geq 0$.

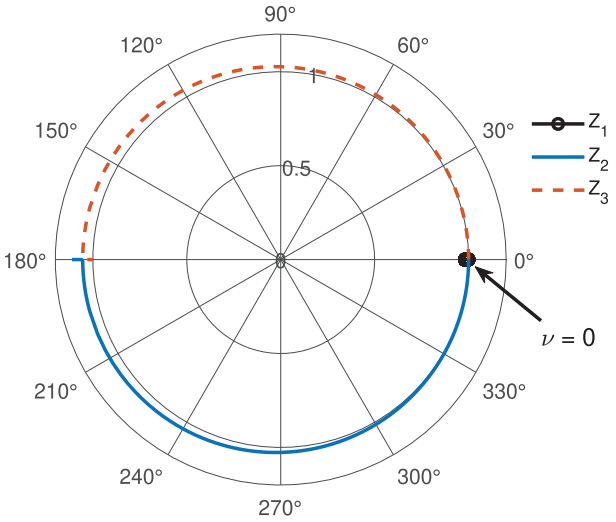


Fig. 2. Root locus of the polynomial $S(Z)$ for $\nu$ varying from 0 to 1.

problem $\Delta_{t,\max}^{\text{CFL}} = \Delta_z/c$. Taking, for instance, $\nu = 0.95$, the resulting time step is $\Delta_t = \nu\Delta_{t,\max}^{\text{CFL}} = 9.5$ fs. Using these data to evaluate the stability conditions in (12), we find that (12b) is not fulfilled since $F(\nu) \simeq -0.9 \not\geq 0$, consequently the simulation will be unstable.

To answer the question of whether there is any value of $\nu$ that makes the simulation stable, the root locus of the stability polynomial $S(Z)$ is shown in Fig. 2 for $\nu$ varying from 0 to 1. It can be seen that for $\nu = 0$, the three roots of $S(Z)$ are equal to the unity. Increasing the value of $\nu$, the root $Z_1$ moves inside the unit circle. However, $Z_2$ and $Z_3$ become a complex-conjugate pair of roots that immediately move outside the unit circle. For $\nu = 1$, $Z_3 = -1$, but $Z_2$ remains outside the unit circle. Therefore, the RK-FDTD method is unstable for all the values of $\nu$.

Despite the unstable nature of the RK-FDTD method, we have carried out the simulation example described above. Fig. 3 depicts the electric field in the whole simulation domain at four different time steps. Fig. 3(a) shows the incident Gaussian pulse traveling toward the graphene sheet at the time step $n = 800$. In Fig. 3(b), the resulting reflected and transmitted pulses can be seen at $n = 1300$. After these pulses have been absorbed by the boundary conditions, the electric field reduces to numerical noise in the whole domain, as shown in Fig. 3(c) for $n = 2000$. The simulation can be finished at this time step with useful results. However, if the simulation continues, the graphene instability leads to a growth of numerical noise, which ends up contaminating the entire domain as shown in Fig. 3(d) for $n = 67000$.

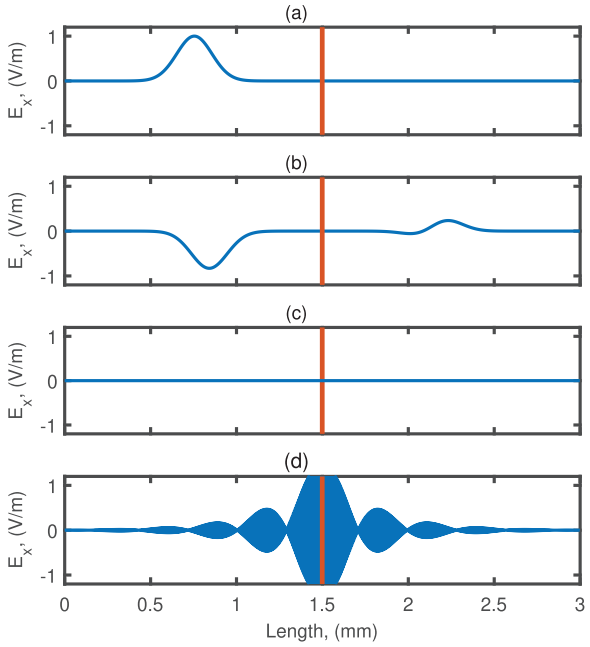


Fig. 3. Electric field snapshots at the time steps (a) $n = 800$, (b) $n = 1300$, (c) $n = 2000$, and (d) $n = 67000$ for a Gaussian pulse impinging normally on an infinite graphene sheet. $\nu = 0.95$.

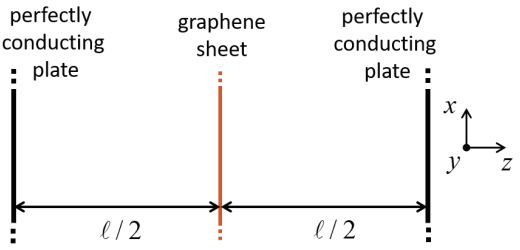


Fig. 4. Graphene-loaded parallel-plate resonator.

As a second example, we consider a 1-D parallel-plate resonator consisting of two perfectly conducting plates in free space separated by a distance $\ell = 24$ $\mu$m. This resonator is loaded with a graphene sheet located at a distance $\ell/2$ from each conducting plate, as shown in Fig. 4.

The exact complex resonant frequencies of this graphene-loaded parallel-plate resonator can be obtained by solving the following characteristic equation:

$$\sin(k\ell) + j\frac{\sigma_0\eta}{2}[1 - \cos(k\ell)] = 0 \tag{13}$$

where $\eta$ is the intrinsic impedance of free space and $k = 2\pi f_c/c$, being $f_c$ the complex resonant frequency. Taking the graphene parameters as $\tau = 0.5$ ps, $\mu_c = 1$ eV, and $T = 300$ K, and solving (13) for the lowest resonance, we obtain $f_c \simeq 7.912 + j0.059$ THz. Thus, the resonant frequency is $f_R = \text{Re}(f_c)$ and the quality factor

$$Q = \frac{\text{Re}(f_c)}{2\text{Im}(f_c)} \simeq 67.$$

To solve this problem using the RK-FDTD method, the space between the two conducting plates is discretized with 160 spatial cells, resulting in a cell size $\Delta_z = 0.15$ $\mu$m. The CFL number is set to $\nu = 1$, so the time step used is $\Delta_t = \Delta_{t,\max}^{\text{CFL}} \simeq 0.5$ fs. The resonator is excited with a Gaussian pulse with an effective maximum frequency of 10 THz. The lowest resonant frequency of the structure is obtained from the first amplitude peak of the discrete Fourier transform (DFT) of the electric field recorded at the position of the graphene sheet. In this communication, the DFT series summation is computed directly instead of applying the fast Fourier transform algorithm [16].

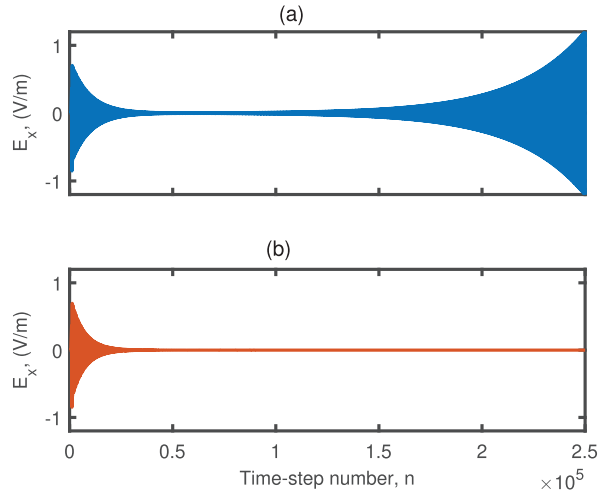


Fig. 5. Electric field recorded at the position of the graphene sheet for the resonator shown in Fig. 4. Results calculated by (a) RK-FDTD and (b) TR-DI-FDTD methods.

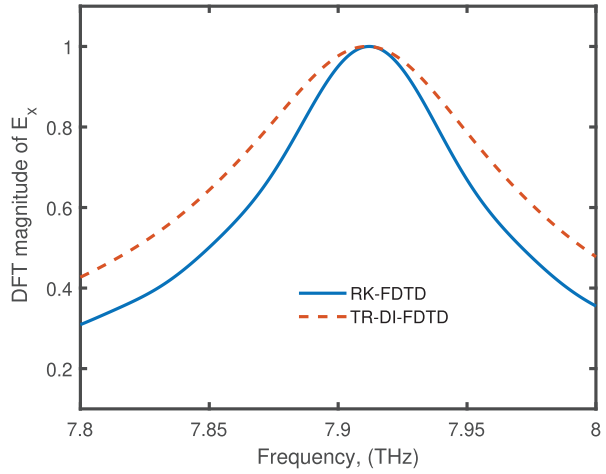


Fig. 6. Normalized DFT magnitude of the time-domain responses shown in Fig. 5.

For this example, it is worth noting that the graphene data and the FDTD parameters are the same as those used in [14, Sec. 6.1], where it was concluded that the RK-FDTD method was stable. This conclusion was drawn by interpreting in [14, Fig. 3] that all the roots of the stability polynomial remain within or on the unit circle as the CFL number varies from 0 to 1. However, according to the stability conditions (12), the simulation should be unstable since $\nu^2 = 1 \not< 1$ and $F(\nu) \simeq -1.0 \not> 0$. In fact, for this example, the magnitudes of the roots of the stability polynomial $S(Z)$ are $|Z_1| \simeq 0.999$, $|Z_2| \simeq 1.011$, and $|Z_3| = 1$. Thus, $Z_2$ lies outside the unit circle in the $Z$ plane.

Fig. 5(a) shows the electric field calculated using the RK-FDTD method over $2.5 \times 10^5$ time steps at the position of the graphene sheet. It can be seen that the electric field decays during the early-time response. However, it begins to increase without bound as the number of time steps exceeds approximately $5 \times 10^4$ steps. For comparison, the same simulation has been repeated using the trapezoidal direct-integration (TR-DI) FDTD method [13]. It can be observed in Fig. 5(b) that this method remains stable for all the time steps.

Despite the unstable behavior of the RK-FDTD method, useful results can still be obtained from the early transient response. To illustrate this idea, Fig. 6 depicts the DFT magnitude of the time-domain responses shown in Fig. 5. The DFT of the RK-FDTD response has been calculated using only the first $5 \times 10^4$ time steps, while the entire time-domain response has been used in the TR-DI-FDTD case. It can be seen that the two methods predict the same resonant frequency $f_R = 7.912$ THz. However, the quality factors are $Q = 114$ and $Q = 79$, which differ appreciably from each other. The higher value of $Q$ obtained with the RK-FDTD method can be understood as a result of the underlying growth (instability) of the electric field computed by this method.

## VI. Conclusion

A stability analysis of the RK-FDTD method for graphene modeling has been carried out. To this end, the von Neumann method has been combined with the RH criterion. It has been found that the RK-FDTD method must satisfy not only the CFL stability limit but also stability conditions involving graphene parameters. Moreover, it has been shown that the RK-FDTD method becomes unstable for commonly used values of these parameters. In fact, no stable graphene parameters have been identified. The theoretical results have been confirmed with numerical examples. In the examples considered, an instability arises in the late-time response. Therefore, it is still possible to obtain some useful results from the early-time response.

## References

[1] A. K. Geim, "Graphene: Status and prospects," *Science*, vol. 324, no. 5934, pp. 1530–1534, Jun. 2009.
[2] G. C. Ghivela and J. Sengupta, "The promise of graphene: A survey of microwave devices based on graphene," *IEEE Microw. Mag.*, vol. 21, no. 2, pp. 48–65, Feb. 2020.
[3] G. W. Hanson, "Dyadic green's functions and guided surface waves for a surface conductivity model of graphene," *J. Appl. Phys.*, vol. 103, no. 6, Mar. 2008, Art. no. 064302.
[4] K. Niu, P. Li, Z. Huang, L. J. Jiang, and H. Bagci, "Numerical methods for electromagnetic modeling of graphene: A review," *IEEE J. Multiscale Multiphys. Comput. Techn.*, vol. 5, pp. 44–58, 2020.
[5] A. Taflove and S. C. Hagness, *Computational Electrodynamics: The Finite-Difference Time-Domain Method*, 3rd ed., Norwood, MA, USA: Artech House, 2005.
[6] V. Nayyeri, M. Soleimani, and O. M. Ramahi, "Modeling graphene in the finite-difference time-domain method using a surface boundary condition," *IEEE Trans. Antennas Propag.*, vol. 61, no. 8, pp. 4176–4182, Aug. 2013.
[7] G. D. Bouzianas, N. V. Kantartzis, C. S. Antonopoulos, and T. D. Tsiboukis, "Optimal modeling of infinite graphene sheets via a class of generalized FDTD schemes," *IEEE Trans. Magn.*, vol. 48, no. 2, pp. 379–382, Feb. 2012.
[8] A. Mock, "Padé approximant spectral fit for FDTD simulation of graphene in the near infrared," *Opt. Mater. Exp.*, vol. 2, no. 6, pp. 771–781, 2012.
[9] H. Lin, M. F. Pantoja, L. D. Angulo, J. Alvarez, R. G. Martin, and S. G. Garcia, "FDTD modeling of graphene devices using complex conjugate dispersion material model," *IEEE Microw. Wireless Compon. Lett.*, vol. 22, no. 12, pp. 612–614, Dec. 2012.
[10] O. Ramadan, "Simplified FDTD formulations for magnetostatic biased graphene simulations," *IEEE Antennas Wireless Propag. Lett.*, vol. 19, no. 12, pp. 2290–2294, Dec. 2020.
[11] F. Moharrami and Z. Atlasbaf, "Stability analysis of the SBC modeling of graphene in the FDTD method," *IEEE Trans. Antennas Propag.*, vol. 69, no. 4, pp. 2421–2426, Apr. 2021.
[12] O. Ramadan, "A note on the stability of the FDTD implementation of the graphene conductivity modeled by a [2/2]-Padé function," *Optik*, vol. 140, pp. 165–170, Jul. 2017.
[13] J. A. Pereda and A. Grande, "A unified view of DI- and ETD-FDTD methods for Drude media," *IEEE Trans. Antennas Propag.*, vol. 70, no. 8, pp. 7334–7337, Aug. 2022.
[14] O. Ramadan, "Investigating the stability of an explicit ADE-FDTD scheme for modeling graphene: Avoiding erroneous conclusions," *Optik*, vol. 275, Feb. 2023, Art. no. 170608.
[15] A. Pereda, L. Vielva, A. Vegas, and A. Iglesias, "Analyzing the stability of the FDTD technique by combining the von Neumann method with the Routh–Hurwitz criterion," *IEEE Trans. Microw. Theory Techn.*, vol. 49, no. 2, pp. 377–381, Feb. 2001.
[16] C. Furse and O. P. Gandhi, "Why the DFT is faster than the FFT for FDTD time-to-frequency domain conversions," *IEEE Microw. Guided Wave Lett.*, vol. 5, no. 10, pp. 326–328, Jan. 1995.